Laughlin, L., Beach, M. A., Morris, K. A., & Haine, J. L. (2014). Optimum single antenna full duplex using hybrid junctions. IEEE Journal of Selected Areas in Communications, 32(9), 1653-1661. [6832460]. 10.1109/JSAC.2014.2330191

Optimum Single Antenna Full Duplex Using Hybrid Junctions

Leo Laughlin, *Member, IEEE,* Mark A. Beach, *Member, IEEE,* Kevin A. Morris, *Member, IEEE,* and John Haine, *Member, IEEE*

***Abstract*—This paper investigates electrical balance (EB) in hybrid junctions as a method of achieving transmitter-receiver (TX-RX) isolation in single antenna full duplex wireless systems. A novel technique for maximizing isolation in EB duplexers is presented, and we show that the maximum achievable isolation is proportional to the variance of the antenna reflection coefficient with respect to frequency. Consequently, antenna characteristics can have a significant detrimental impact on the isolation bandwidth. Simulations which include embedded antenna measurements show a mean isolation of 62dB over a 20MHz bandwidth at 1.9GHz, but relatively poor performance at wider bandwidths. Furthermore, the operational environment can have a significant impact on isolation performance. We present a novel method of characterizing radio reflections being returned to a single antenna. Results show as little as 39dB of attenuation in the radio echo for a highly reflective indoor environment at 1.9GHz, and that the mean isolation of an EB duplexer is reduced by 7dB in this environment. A full duplex architecture exploiting electrical balance is proposed.**

***Keywords*—Duplexers, Full-duplex, Hybrid junctions, Interference cancellation, Self-interference.**

I. Introduction

WIRELESS COMMUNICATION systems are fundamentally limited by the availability of the electromagnetic spectrum in which they must operate. Consequently, increasing spectral efficiency has been a major focus of research over recent decades, and given the exponential growth in demand for radio services, spectral efficiency will continue as a key research driver for years to come. Radio signals attenuate quickly with distance, and therefore in radio systems the transmit signal powers are typically much higher than receive signal powers (often over 100dB higher in cellular systems). Because of this, it has long been held that a radio system cannot transmit and receive on the same frequency at the same time, as the high powered transmit signal would lead to catastrophic self-interference at the receiver. In current radio systems, full duplex operation is achieved by simply avoiding this problem. Spectral resources are divided between the transmit and receive channels either in time, using Time Division Duplexing (TDD), or frequency, using Frequency Division Duplexing (FDD). However, since the 1980s [1], [2], and particularly in recent years [3]–[8], research has challenged this paradigm, proposing new system architectures utilizing various techniques to provide high levels of transmit to receive isolation, thus allowing simultaneous transmission and reception at the same frequency. This division free duplexing, often referred to simply as full duplex wireless, has obvious benefits for spectral efficiency, theoretically providing double the capacity of TDD or FDD systems without increasing bandwidth.

To achieve in-band full duplex communication, the self-interference must be reduced to an acceptable level at the receiver. Any residual self-interference will effectively increase the receiver noise floor, reducing the capacity of the receive channel. To achieve the theoretical two-fold capacity increase, infinite isolation would be required. Infinite TX-RX isolation is not practically feasible; however, provided the isolation is high enough such that the residual self-interference is at least some 5dB or so below the receiver noise floor, then the impact on the receive performance will be negligible. For an LTE handset, with a maximum transmit power of 23dBm, and a receiver noise floor of around -95dBm, then 23dBm - (-95dBm) + 5dB = 123dB would be required to reduce the self-interference to 5dB below the level of the noise floor. For a typical Wi-Fi system, a similar calculation tells us that approximately 115dB of isolation would be required. These high levels of isolation are not easily achievable, however even if the residual self-interference noticeably increases the receiver SNR and thereby reduces the channel capacity, there may still be a net capacity gain in operating two simultaneous reduced capacity channels in full duplex over the self-interference free TDD alternative.

Existing designs [2]–[6], [9]–[11], involve various combinations of analog cancellation, digital cancellation, and antenna based suppression to provide the high level of isolation required. Digital cancellation [6], [7], [11]–[13], although effective and easy to implement in baseband DSP, cannot prevent self-interference from overloading the receiver front end, which would prevent any recovery of the receive signal. Analog cancellation [4]–[6], [8], [10], [14], [15], can provide significant isolation prior to the receiver, reducing self-interference and preventing receiver overloading, making it a requirement in most practical systems [4]. Significant progress has also been made in understanding the impact of hardware limitations and other imperfections on system performance [16]–[19], and network capacity and MAC protocols for full duplex networks have also been the subject of investigation [8], [12], [20]–[23].

Leo Laughlin, Mark Beach, and Kevin Morris are with the Department of Electrical and Electronic Engineering, University of Bristol, UK, BS8 1UB e-mail: Leo.Laughlin@bristol.ac.uk.

John Haine is with u-blox AG, Zürcherstrasse 68, 8800 Thalwil, Switzerland

Manuscript received October 15, 2013; revised March 27, 2014.

This research is supported by the UK Engineering and Physical Sciences Research Council (EP/I028153/1) through the Centre for Doctoral Training in Communications, and through iCASE sponsorship by u-blox AG.

Antenna based suppression methods can provide significant isolation, however these designs require additional antennas which is a disadvantage in applications where device size and form factor are important considerations. Antenna separation [2], [6], [8], [11], [12], uses separate transmit and receive antennas and is a simple and effective method of achieving TX-RX isolation. Shielding, radiation pattern, and polarization can be exploited to improve isolation [8], [24], [25], however the achievable isolation is fundamentally limited by the physical separation of the antennas. Antenna cancellation [3], [5], [26], [27] involves positioning transmit antennas such that their radiated signals interfere destructively at the receive antenna(s). Although effective, the isolation offered by this technique is significantly reduced in multipath environments [3]. Transmit beamforming in MIMO systems with antenna separation [9], [17], [28], can also be exploited to reduce self-interference at the receive antennas, and can be combined with spatial multiplexing, although obtaining interference suppression in this way consumes spatial degrees of freedom that could have otherwise been used for data transmission [17].

In many applications, and especially in consumer products, cost reduction and form factor often take precedence over radio performance. The multi-antenna techniques mentioned above are well suited to applications such as cellular basestations, however the increase in device cost and size due to the additional antennas make these techniques less attractive for smaller devices such as smartphones and tablet computers. Single antenna full duplex systems have been reported in [4], [29]. These implementations use circulators to provide some level of TX-RX isolation (around 15-20dB) in the antenna coupling network, however, circulators are also an unattractive option due to their cost, size, and limited bandwidth.

In this paper, we study electrical balance (EB) using hybrid junctions as a possible alternative method for providing TX-RX isolation in full duplex system. This technique has been shown to provide high TX-RX isolation over wide bandwidths [30], [31], however this method requires just one antenna, reducing device size and cost compared to an antenna separation or antenna cancellation system. In section II, we review Electrical Balance Isolation techniques, and in section III, we derive expressions for the optimum balancing impedance and the maximized isolation, and show that practical antennas will limit performance. Section IV then analyzes the performance of an EB duplexer with dipole antenna using the novel optimal balancing technique. In section V the impact on isolation performance due to radio reflections in the environment is investigated, and section VI discusses possible system architectures exploiting EB duplexing.

II. Electrical Balance Duplexing

Transformer based isolation methods were first developed in the early 20th century for use in wired telephony systems, which, incidentally, are themselves early examples of on-frequency full duplex systems. In an analog telephone, the microphone and earpiece must both be connected to the telephone line, but the microphone signal must be isolated from the earpiece to prevent the users own speech deafening them

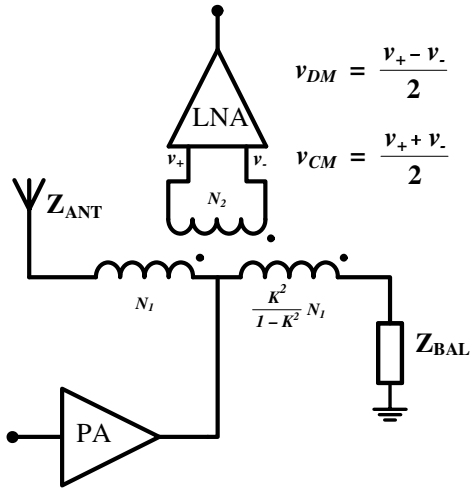

Fig. 1. Hybrid transformer providing TX-RX isolation using electrical balance, and definitions of the common mode signal, v_{CM}, and differential mode signal v_{DM}, at the LNA input.

to the much weaker audio signal being received. This early application is entirely analogous to the requirements of single antenna full duplex wireless transceivers, where the TX and RX must both be coupled to the same antenna, but high TX-RX isolation is required. This circuit technology is commonplace in wired communication, and the hybrid junction is widely used in RF engineering. Recent research has investigated using electrical balance in hybrids for implementing wireless FDD [30]–[35], where it could potentially replace the multiple off-chip acoustic resonator duplexers required for FDD operation in todays multiband cellular handsets, thus reducing their cost and size. This technique, sometimes referred to as electrical balance isolation (EBI) is, however, equally applicable to the full duplex wireless systems discussed presently, although for full duplex operation the isolation requirements are much higher than for FDD.

EB duplexing exploits electrical balance in a hybrid junction to achieve high TX-RX isolation. A number of transformer configurations can be used, including auto-transformers [36], [37], 90 or 180 hybrid couplers [1], [34], and hybrid transformers [31]. Fig. 1 [31] depicts a hybrid transformer based EB duplexer and defines the Differential Mode (DM), and Common Mode (CM) signals at the receiver input. EB duplexers must not only provide high DM isolation in order to reduce self-interference, but must also protect the receiver from CM signals, which can cause Low Noise Amplifier (LNA) device breakdown due to the large voltage swing at the LNA input. In [36], a prototype auto-transformer based duplexer has been shown to provide a 60dB isolation bandwidth (the bandwidth over which at least 60dB of isolation is achieved) of over 50MHz for DM signals, however this architecture provides no CM isolation, making it unsuitable for all but low transmit power applications. Hybrid transformer based implementations, however, can provide CM isolation, making them preferable for most modern wireless applications.

The operation of the EB duplexer depicted in Fig. 1 is

analyzed in detail in [31]. The TX current supplied by the Power Amplifier (PA) enters the hybrid at the center tap of the primary winding and is split between two paths flowing in opposite directions, with one component flowing to the antenna (and being transmitted), and the other to the balancing network. The relative magnitudes of these currents is determined by the coupling coefficient, K. The balancing impedance is adjusted such that these two currents create equal but opposite magnetic fluxes that cancel, and therefore zero current is induced in the secondary winding and the receiver is completely isolated from the transmitter. Conversely, a signal received by the antenna causes current to flow through the primary winding in one direction, thereby coupling it to the receiver winding. There is, of course, some loss associated with the duplexer. Some TX power is dissipated by the balancing network, instead of being transmitted, and not all of the RX power is coupled to the LNA. The losses of the TX and RX paths can be traded off against one another by changing the coupling coefficient, and when $K^2 = 0.5$ the losses of the TX and RX paths are both 3dB. Although any loss in the TX and RX paths degrades efficiency and sensitivity respectively, the magnitude of these losses is comparable to the losses observed in alternative architectures, such as the loss due to the circulator, splitter, and coupler used for analog cancellation in [4].

It can be shown [38] that the DM TX-RX power gain of an ideal EB duplexer is

$$G_{TX-RX} = L\left|\Gamma_{BAL} - \Gamma_{ANT}\right|^2 \tag{1}$$

where Γ_{BAL} and Γ_{ANT} are the complex reflection coefficients of the balancing network and antenna respectively, and where L is a constant scaling factor which depends on the coupling coefficient such that $L = K^2(1-K^2)$. As we can see from (1), in the ideal circuit, the isolation depends on how closely Γ_{BAL} can match Γ_{ANT}, and hence how closely the balancing impedance can match the antenna impedance. Results in [30] also demonstrate that (1) remains valid for the non-ideal circuit, and that parasitic elements in the hybrid transformer have little effect on DM isolation compared to balancing inaccuracies. However, due to environmental effects, Γ_{ANT} may be time variant and therefore, as is also the case with analog cancellation, the system must be adaptive.

Although the non-ideal properties of the hybrid have little impact on the DM isolation, parasitic coupling can significantly reduce the CM isolation. In [30], a fully differential EB duplexer is introduced which exploits differential TX inputs to cancel the CM signal at the LNA. Although providing significantly higher CM isolation than single ended EB duplexers, the additional balun required to couple the antenna increases loss in the receive path, thereby adding to the noise figure. In both differential and single ended EB duplexers, the DM TX-RX gain is given by (1), and therefore the analysis presented in this paper is applicable to all of the EB duplexer architectures discussed presently.

III. Achievable Isolation

In order to obtain high isolation, the balancing impedance must be as close as possible to the antenna impedance. For purely resistive loads, high isolation can be achieved over wide bandwidths, however, in practice the antenna impedance seen by the hybrid transformer is frequency dependent. Previous work [30], [31] has demonstrated the achievable isolation using near ideal 50Ω impedances to model the antenna. In this paper we investigate the reduction in isolation performance when a real antenna is used, strategies for calculating the balancing impedance, and we calculate the optimum balancing impedance for an arbitrary antenna and the maximum isolation that this can achieve.

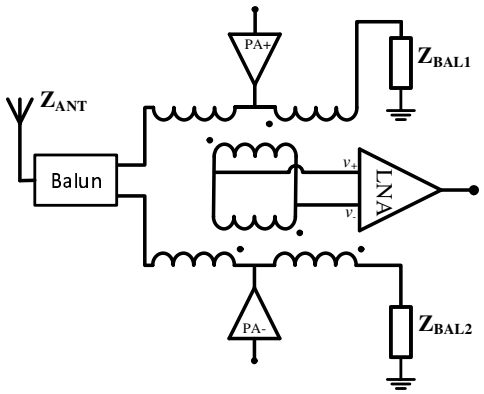

Fig. 2. Differential EB duplexer [30].

A. Balancing at the Carrier Frequency

Considering the case where the antenna reflection coefficient is a frequency selective function, $\Gamma_{ANT}(\omega)$, and Γ_{BAL} is frequency invariant, the frequency dependent TX-RX power gain of the duplexer is given by

$$G_{TX-RX}(\omega) = L\left|\Gamma_{BAL} - \Gamma_{ANT}(\omega)\right|^2. \tag{2}$$

A simple but naive method of determining the balancing impedance is to set it to be equal to the antenna impedance at the carrier frequency, ω_c, such that

$$\Gamma_{BAL} = \Gamma_{ANT}(\omega_c). \tag{3}$$

Although this provides very high (theoretically infinite) isolation at the carrier frequency, variation in the antenna impedance with frequency drastically reduces the isolation as we move away from this frequency. Since the self-interference power is spread across the transmit bandwidth, setting the balancing impedance to obtain high isolation at a single frequency point is not necessarily useful if this results in poor isolation at other frequencies in the transmit band. Instead, we wish to maximize the SNR at the receiver, and therefore we wish to find the optimum balancing impedance which minimizes the total self-interference power across the entire band.

B. Optimum Balancing Impedance

To minimize the self-interference power at the LNA, we must minimize the mean of the TX-RX gain as given by (2)

across the band of interest (e.g. the transmit signal bandwidth). Here we may note that this is a minimum mean square error (MMSE) problem, and assuming the balance impedance is frequency invariant (see below), we may write the minimum TX-RX gain, $G_{TX-RX_{MMSE}}$, as

$$G_{TX-RX_{MMSE}} = \min_{\Gamma_{BAL}} \left\{ \overline{L\left|\Gamma_{BAL} - \Gamma_{ANT}(\omega)\right|^2} \right\} \quad \text{for} \quad \omega_l < \omega < \omega_h \tag{4}$$

$$= L \min_{\Gamma_{BAL}} \left\{ \frac{1}{\omega_h - \omega_l} \int_{\omega_l}^{\omega_h} \left|\Gamma_{BAL} - \Gamma_{ANT}(\omega)\right|^2 d\omega \right\} \tag{5}$$

where ω_h and ω_l are the upper and lower band limits respectively. It can be shown that the minimizer, $\Gamma_{BAL_{MMSE}}$, is given by

$$\Gamma_{BAL_{MMSE}} = \frac{1}{\omega_h - \omega_l} \int_{\omega_l}^{\omega_h} \Gamma_{ANT}(\omega) \quad d\omega \tag{6}$$

$$= \overline{\Gamma_{ANT}(\omega)} \qquad \text{for} \quad \omega_l < \omega < \omega_h \tag{7}$$

and therefore, in the case where the balancing network is a single complex impedance, the balancing impedance which minimizes the self-interference at the receiver across a given frequency band is that which occurs when the balancing reflection coefficient equals the mean of the antenna reflection coefficient across that band. The optimum balancing impedance, $Z_{BAL_{MMSE}}$, is therefore given by

$$Z_{BAL_{MMSE}} = Z_0 \frac{1 + \overline{\Gamma_{ANT}(\omega)}}{1 - \overline{\Gamma_{ANT}(\omega)}} \quad \text{for} \quad \omega_l < \omega < \omega_h \tag{8}$$

where Z_0 is the normalizing impedance. At this optimum point, the TX-RX isolation is maximized and is given by

$$G_{TX-RX_{MMSE}}(\omega) = L|\Gamma_{BAL_{MMSE}} \quad - \quad \Gamma_{ANT}(\omega)|^2 \tag{9}$$

$$G_{TX-RX_{MMSE}}(\omega) = L|\overline{\Gamma_{ANT}(\omega)} \quad - \quad \Gamma_{ANT}(\omega)|^2 \quad \text{for} \quad \omega_l < \omega < \omega_h \tag{10}$$

and the minimized mean gain (i.e. the maximized mean isolation) across the band is

$$\overline{G_{TX-RX_{MMSE}}(\omega)} = L\overline{|\overline{\Gamma_{ANT}(\omega)} - \Gamma_{ANT}(\omega)|^2} \quad \text{for} \quad \omega_l < \omega < \omega_h. \tag{11}$$

Here we may note that the maximized mean isolation for a given frequency band is proportional to $\overline{|\overline{\Gamma_{ANT}(\omega)} - \Gamma_{ANT}(\omega)|^2}$, which is the variance with respect to frequency of the antenna reflection coefficient $\Gamma_{ANT}(\omega)$ over said band. This result is intuitive, and quantifies our earlier observation that variations in the antenna reflection coefficient over frequency will limit the isolation bandwidth.

C. Balancing Impedance Realisation

The balancing impedance can be realized using a series RC or RL circuit, depending on the sign of the imaginary part of the balance impedance (thus requiring both configurations to be available in the balancing network). Here we may recall the assumption that the balancing impedance is frequency invariant. However, a frequency invariant complex impedance cannot be physically realized by any RLC network. Nonetheless, in general this analysis remains valid as in comparison to the practical variation in antenna impedance, a first order RC or RL circuit impedance can be assumed to be frequency flat over typical system bandwidths. Furthermore, it is pertinent to note that this analysis assumes that delay (linear phase shift) in the antenna impedance (due, for example, to a transmission line or cable between the duplexer and antenna) is compensated for by an equal delay in the balancing network.

IV. Performance Analysis

RF simulation was used to determine the performance of the circuit in Fig. 1 with a real antenna connected to the duplexer, and to investigate the impact of the different balancing strategies. Measured S_{11} frequency response data taken from a real antenna was incorporated into the circuit simulator, thereby creating an almost perfect model of the antenna reflection within the simulation (limited only by the Vector Network Analyzer (VNA) measurement accuracy and quantization). A lumped element model of the transformer was used to simulate the reduced magnetic coupling and quality factor. This model used the parameters of the transformer which was fabricated in [30], in which the primary and secondary winding inductances, L_1 and L_2, are 2.24nH and 15.3nH respectively, the quality factors of the primary and secondary windings, Q_1 and Q_2 , are 10.5 and 14.6 respectively, and L_1 is the winding on the PA side. The coupling coefficient, K, is 0.84, and the tapping ratio is 1:1. In the simulation the balancing impedance was implemented as a series RC (or RL, see above) circuit.

Fig. 3 shows the simulated isolation performance for the two different balancing strategies when a dipole antenna is connected. When carrier frequency balancing is used, high isolation is obtained at the carrier frequency, but quickly reduces either side of this, and in this case the system has a 50dB isolation bandwidth of only 10MHz. When MMSE balancing is used, the peak isolation is traded for better average isolation across the system bandwidth, and this extends the 50dB isolation bandwidth to 38MHz. The simulation was also used to compare the isolation when using the RC balancing network against the isolation which would occur if using the non-realizable frequency flat complex impedance which was assumed in the derivation. In all simulations conducted, the RC or RL balanced case was found to be in close agreement with the frequency invariant balancing case, showing less than 1dB difference in mean isolation, thus validating the narrowband assumption. The results also demonstrate that the variation in antenna impedance has a profound effect on the isolation bandwidth. Even when the MMSE balancing is used, the 50dB isolation bandwidth seen here is substantially less than the >250MHz 50dB isolation bandwidth reported in [30] where

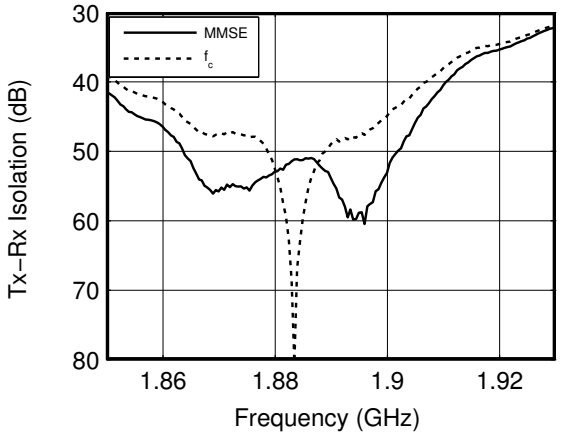

Fig. 3. Simulated TX-RX isolation of the EB duplexer with a dipole antenna when balancing at the carrier frequency, and when using MMSE balancing. Carrier balancing is maximizing the isolation at 1.833GHz. The MMSE balancing is maximizing the isolation for a 30MHz bandwidth centered at the same frequency.

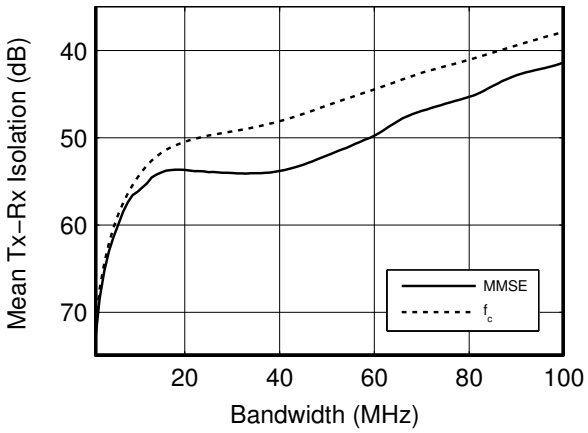

Fig. 4. Simulated mean TX-RX isolation for different system bandwidths up to 100MHz for both balancing strategies.

a 50Ω load was used instead of an antenna, and this suggests that previously reported duplexer isolation performance figures in [30], [31] are not practically achievable. Fig. 4 compares simulated mean isolation for system bandwidths up to 100MHz when using carrier frequency balancing, and when using MMSE balancing to minimize self-interference over that particular system bandwidth. In both cases the variation in antenna impedance increases with bandwidth, thereby reducing the isolation, however at wider bandwidths the MMSE balancing results in up to 5dB of additional interference suppression compared to carrier balancing.

V. Effect of the Propagation Environment

It has been shown that frequency variation in the reflection coefficient at the antenna port limits the isolation bandwidth provided by the EB duplexer, however we have thus far not considered the mechanism by which this energy is reflected. We can, in fact, divide the reflected energy into two components: energy reflected by the antenna system itself, and energy reflected by the environment in which the antenna operates. In the case of the latter, transmit energy leaves the antenna, and is reflected back into the antenna by nearby objects. We may refer to this as the *radio echo*. Since we have shown that the antenna S_{11} is a critical factor in determining the performance of an EB duplexer, then, if powerful enough, the environmental reflections are likely to affect the isolation performance. In this section we measure the power of these reflections in two different environments and quantify the effect this has on the EB duplexer isolation.

A. Radio Echo Measurement

We may express the reflection at the antenna port as the sum of the reflection due to the antenna system itself, $\Gamma'_{ANT}(\omega)$, and the radio echo, $\Gamma_{ECHO}(\omega)$, and hence

$$\Gamma_{ANT}(\omega) = \Gamma'_{ANT}(\omega) + \Gamma_{ECHO}(\omega). \tag{12}$$

The echo component, $\Gamma_{ECHO}(\omega)$, at a particular position could be determined by measuring $\Gamma_{ANT}(\omega)$ at that position, and then subtracting an estimate of $\Gamma'_{ANT}(\omega)$, which could be obtained by measuring the antenna reflection coefficient in an anechoic chamber, such that

$$\Gamma_{ECHO}(\omega) \approx \Gamma_{ANT}(\omega) - \Gamma_{ANECHOIC}(\omega) \tag{13}$$

where

$$\Gamma_{ANECHOIC}(\omega) \approx \Gamma'_{ANT}(\omega). \tag{14}$$

This method would estimate the full frequency response of the reflection channel, but has the drawback of requiring the use of an anechhoic chamber. Another possible method for estimating the environmental echo power is to observe the S_{11} impulse response in the time domain by taking the inverse discrete Fourier transform (IDFT) of the S_{11} frequency response. This approach has been successfully used in [25] to investigate environmental effects on the self-interference channel in an antenna separation full duplex system. This transform based method, however, requires a significant measurement bandwidth in order to resolve the reflection components to the required time domain resolution (typically $\sim$10ns or less for indoor environments), and is thus not possible when the measurement bandwidth is sufficiently limited by the antenna bandwidth. Furthermore, even when windowing is correctly applied, the time domain "ringing" (i.e sidelobes) caused by the finite measurement bandwidth is particularly problematic in an S_{11} measurement, as the environmental components can be obscured by ringing from the much larger $\Gamma'_{ANT}(\omega)$ reflection component, further necessitating a wide measurement bandwidth. Here we present an alternative narrowband technique which estimates the mean echo power at a single given frequency, and does not require the use of an anechioc chamber.

B. Estimating the Echo Power Statistically

By making some basic assumptions regarding the nature of the reflected signals it is possible to estimate the loss of the

echo channel for a given environment at a given frequency as follows. Firstly, let us assume that the reflection due to the antenna, $\Gamma'_{ANT}(\omega)$, is stationary in time. Since the antenna is a fixed physical device its response is, generally speaking, time invariant. Minor variations in the antenna reflection coefficient may occur due to changes in temperature and device ageing effects, however these occur over relatively long timescales and can therefore be neglected. If we take a time domain measurement of the reflection coefficient at the carrier frequency, $\Gamma_{ANT}(\omega_c, t)$, as the antenna moves through the environment, then under the above assumption any variation in the measured reflection coefficient over time is due to the radio echo component. Hence we may write

$$\Gamma_{ANT}(\omega_c, t) = \Gamma'_{ANT}(\omega_c) + \Gamma_{ECHO}(\omega_c, t). \quad (15)$$

Secondly, let us assume that the equivalent baseband radio echo is a zero mean fading process [39], such that

$$\Gamma_{ECHO}(\omega_c, t) = \eta(0, \sigma_E^2) \quad (16)$$

and the reflection at the antenna can therefore be written as

$$\Gamma_{ANT}(\omega_c, t) = \Gamma'_{ANT}(\omega_c) + \eta(0, \sigma_E^2). \quad (17)$$

where $\eta(0, \sigma_E^2)$ is some arbitrary distribution with zero mean and variance σ_E^2. Since we have assumed the fading process in the echo channel is zero mean, σ_E^2 is equal to the average power gain of the echo channel

$$\overline{|\Gamma_{ECHO}(\omega_c, t)|^2} = \sigma_E^2. \quad (18)$$

Furthermore, since $\Gamma'_{ANT}(\omega_c)$ is time invariant, this is also the variance of $\Gamma_{ANT}(\omega_c, t)$

$$\overline{|\Gamma_{ECHO}(\omega_c, t)|^2} = var\left\{\Gamma_{ANT}(\omega_c, t)\right\} \quad (19)$$

and hence the variance of a time domain measurement of the reflection coefficient at a given frequency, taken as the antenna moves through the environment, provides an estimate of the mean radio echo power at that frequency averaged over the measurement path. Alternatively, one could also interpret this estimation method as assuming the reflection at the antenna port is a Ricean channel, and inferring the echo component by estimating the K-factor. Although requiring measurement at only a single frequency and thus being suitable for use with narrowband antennas, this method does not give any insight into how this power is spread in the time domain. Conversely, the wideband IDFT method used in [25] can provide useful information such as the RMS delay spread. Estimating the reflected power at a single frequency may also be advantageous in environments where radio reflections are highly frequency dependent, and this technique could also be repeated at multiple frequency points to estimate the amplitude frequency response of the environmental reflection channel.

C. Measurement

In order to use the method described above to measure the additional reflection at the antenna port due to radio echoes, it is necessary to ensure that the conditions these are based upon are valid. Specifically, to obtain a valid estimate, it is necessary to ensure that the radio echo channel is fading, and therefore the antenna must be moving whilst the measurement is taken. However, movement in cables can be a significant source of measurement error, and to mitigate against this, high quality phase stable cables were used in this measurement. Additionally, to minimize any cable movement, and to allow the antenna position to be easily controlled without interfering with the measurement (as would be the case if moving the antenna by hand), a special jig was constructed to perform the measurement. The antenna was mounted on the end of a 2m wooden pole, which was attached to a pivot mounted next to a VNA. This allowed the antenna to be easily moved as the measurement was taken, and, since the measurement apparatus described does not move relative to the antenna, it does not introduce any extra variation in the reflected signal, and therefore does not interfere with the measurement. The antenna was swept through a distance of approximately 2.5m in the center of the room, taking care that the antenna did not come unduly close to any reflective objects which might distort the measurement. At the 1.9GHz measurement frequency this meant that measurement was performed over a distance greater than 15 wavelengths.

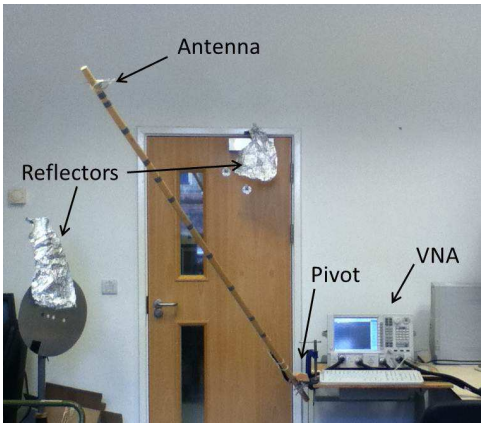

Fig. 5. The radio echo measurement setup in the laboratory.

Two environments were measured: a rich multipath environment in the laboratory, and a less reflective home environment. The laboratory has many reflective surfaces, including a metal raised floor, metal heating ducts in the ceiling cavity, and various metal pieces of lab equipment. Furthermore, steel plate and tin-foil reflectors were placed around the laboratory to increase the reflectivity of the environment. Conversely, the home environment does not have many metal surfaces or objects, and it is therefore reasonable to expect there to be a lower radio echo power in this environment. A Taoglas PA.710 multiband cellular antenna was used in these experiments, as this is representative of a typical cellular or WLAN antenna.

D. The Effect of the Environment on isolation

In addition to estimating the echo power in the home and laboratory environments, the antenna S_{11} frequency response was also measured at these locations. It is important to note

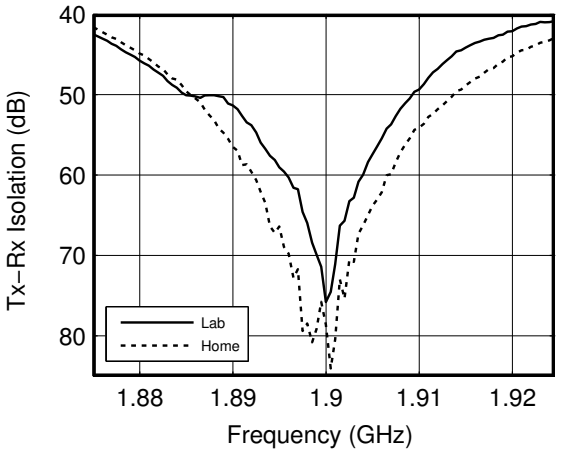

Fig. 6. The TX-RX isolation of the EB duplexer optimized for maximum isolation over a 20MHz bandwidth in two different propagation environments.

TABLE I. SUMMARY OF MEASURED RADIO ECHO POWER AND EB DUPLEXER PERFORMANCE IN THE HOME AND LABORATORY ENVIRONMENTS.

Environment	Lab	Home
Echo Atten.	-39dB	-49dB
Mean Isol (20MHz BW)	-55dB	-62dB
60dB isol. BW	8MHz	14MHz
R	78.5Ω	45.7Ω
L	0.8 nH	1.8 nH

that an S_{11} measurement is a measure of total reflection at the antenna port, regardless of the reflection mechanism. The measured antenna S_{11} therefore also includes any radio echoes from the environment. Consequently, by incorporating measured antenna S_{11} data from the home and lab environments into the simulation, it was possible to realistically simulate the antenna *and the echo channel*, and thereby investigate the impact of the different propagation environments on the performance of the duplexer. Table I summarizes the measured echo power and simulated isolation performance of the duplexer at two example locations in the home and lab environments, and shows component values for series RL or RC circuits required to implement the balancing impedance. The echo channel attenuation is as little as 39dB for the reflective lab environment. Considering the high isolation requirements, clearly this means that the returning echo signals are powerful enough to have an effect on performance. Since the radio echoes are included as part of S_{11} measurement the optimum balance calculation takes this component into account, maximizing the isolation for any given antenna and environment. However, comparing the optimum isolation performance in the two environments (Fig. 6 and Table I), we can see that the radio echoes have a significant impact on the maximum achievable isolation, with mean isolation over the bandwidth reducing by 7dB due to the additional radio echo in the lab. A further observation is that required resistor values show a relatively large variation. This has negative implications for the hardware design of the tunable balancing impedance, as a requirement for a large tuning range and high accuracy in the balancing network would increase system complexity.

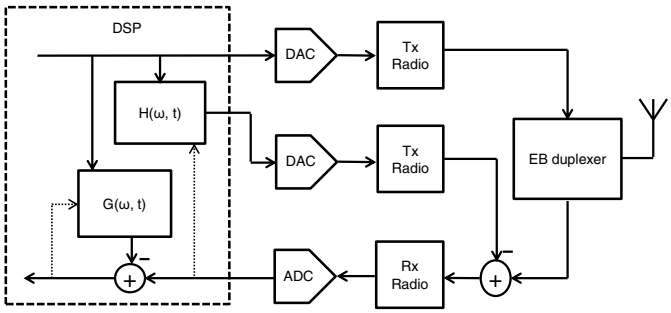

Fig. 7. Possible architecture for a single antenna full duplex radio system incorporating an electrical balance and analog cancellation (EBAC), and digital baseband cancellation.

VI. FULL DUPLEX SYSTEM ARCHITECTURE

Fig. 7 shows a possible single antenna full duplex system architecture exploiting electrical balance, analog cancellation, and digital cancellation. This electrical balance and analog cancellation (EBAC) RF transceiver architecture is similar to systems reported in [8], [10], but in this system a single antenna connected via an EB duplexer is used in place of the separate transmit and receive antennas. Similarly, the EB duplexer could be used instead of the circulator in [4]. For practical antenna separations possible in laptop sized devices, the EB duplexer can provide TX-RX isolation exceeding antenna separation for bandwidths of 20MHz or less [8]. Given that EB duplexing can outperform antenna separation in this scenario, it is reasonable to expect that the proposed EBAC architecture would meet or exceed the antenna separation and analog cancellation (ASAC) isolation observed in [8]. Similarly, one would also expect EB duplexing to be compatible with digital cancellation in the same manner as other analog suppression techniques. Further work is required to investigate the design and performance of full duplex system architectures incorporating EB duplexing.

VII. CONCLUSION

Electrical balance in four port hybrid junctions can be exploited to obtain TX-RX isolation in single antenna full duplex systems. Unlike alternative multi-antenna techniques, such as antenna separation and antenna cancellation, the isolation is not limited by the physical separation of the antennas, making this technique highly applicable where small device size and form factor are important design considerations. The EBI based solution is also tunable over a wide frequency range, and can potentially be implemented using integrated circuit technology [30], [31].

It has been shown that TX-RX isolation can only be obtained when the balancing impedance closely matches the antenna impedance, thus limiting the isolation bandwidth. The simulated duplexer described in section IV, with embedded physical

antenna data, provides on average 62dB of isolation across a 20MHz bandwidth, however, this is significantly reduced at wider bandwidths. Conversely, antenna separation does not limit bandwidth, and circulator based systems have been shown to maintain isolation over wide bandwidths [4].

In section III we introduce an MMSE balancing technique for minimizing the self-interference power over the system bandwidth. When MMSE balancing is achieved, the residual self-interference is proportional to the variance of the antenna S_{11} frequency response. The results presented show that MMSE balancing can significantly extend the isolation bandwidth compared to balancing the system at the carrier frequency, with a near four-fold increase in 50dB isolation bandwidth being observed. However, even with MMSE balancing, the isolation bandwidth of the duplexer is significantly degraded by the antenna.

The radiated energy reflected back into the antenna in indoor environments has been shown to reduce the achievable isolation bandwidth. A novel method of estimating radio echo power has been presented in section V, and using this technique the radio echo power in two environments has been measured. Results show 39dB of attenuation in the echo channel for a relatively reflective indoor environment. Any radio echoes are part of the observed antenna S_{11}, and thus can increase the S_{11} variance, thereby further reducing the isolation bandwidth of an EB duplexer.

Electrical balance duplexing could potentially be combined with analog cancellation, digital cancellation, and full duplex MIMO [3], [21] where EB duplexing has the potential to reduce the number of required antennas by half. The design and implementation of full duplex radio systems incorporating electrical balance requires much further investigation.

ACKNOWLEDGMENT

The authors would like to thank Chris Marshall and Mici McCullagh of u-blox for insightful technical discussions, and Taoglas for their generosity in proving the antennas used in this research.

REFERENCES

[1] C. K.Richardson, "Improvements in or relating to transmitters/receivers," UK Patent 1 577 514, Oct., 1980.

[2] S.Chen, M. A.Beach, and J. P.McGeehan, "Division-free duplex for wireless applications," *Electron. Lett.*, vol. 34, no. 2, pp. 147–148, 1998.

[3] E.Aryafar, M. A.Khojastepour, and S.Rangarajan, "MIDU: Enabling MIMO Full Duplex," in *Proc. ACM Int. conf. Mob. Comput. Netw.*, 2012, pp. 257–268.

[4] D.Bharadia, E.McMilin, and S.Katti, "Full Duplex Radios," in *Proc. 2013 ACM SIGCOMM*, Hong Kong, 2013.

[5] J. I.Choi, M.Jain, K.Shrinivasan *et al.*, "Achieving Single Channel, Full Duplex Wireless Communication," in *Proc. ACM Int. conf. Mob. Comput. Netw.*, Chicago, IL, 2010, pp. 1–12.

[6] M.Duarte, C.Dick, and A.Sabharwal, "Experiment-Driven Characterization of Full-Duplex Wireless Systems," *Wirel. Commun. IEEE Trans.*, vol. 11, no. 12, pp. 4296–4307, 2012.

[7] M. A.Khojastepour and S.Rangarajan, "Wideband digital cancellation for full-duplex communications," in *Signals, Syst. Comput. (ASILOMAR), 2012 Conf. Rec. Forty Sixth Asilomar Conf.*, 2012, pp. 1300–1304.

[8] A.Sahai, G.Patel, A.Sabharwal *et al.*, "Pushing the limits of full duplex wireless: design and real-time implementation," Rice Univ. Houston, TX, Tech. Rep. TREE1104, 2009. [Online]. Available: http://arxiv.org/abs/1107.0607

[9] D. W.Bliss, P. A.Parker, and A. R.Margetts, "Simultaneous Transmission and Reception for Improved Wireless Network Performance," in *Stat. Signal Process. 2007. SSP '07. IEEE/SP 14th Work.*, 2007, pp. 478–482.

[10] J.Lee, "Self-Interference Cancellation using Phase Rotation in Full Duplex Wireless," *Veh. Technol. IEEE Trans.*, vol. PP, no. 99, p. 1, 2013.

[11] M.Duarte and A.Sabharwal, "Full-duplex wireless communications using off-the-shelf radios: Feasibility and first results," in *Signals, Syst. Comput. (ASILOMAR), 2010 Conf. Rec. Forty Fourth Asilomar Conf.*, 2010, pp. 1558–1562.

[12] M.Jain, J. I.Choi, T. M.Kim *et al.*, "Practical Real-Time Full Duplex Wireless," in *Proc. ACM Int. conf. Mob. Comput. Netw.*, Las Vegas, NV., 2011, pp. 301–312.

[13] A.Frotzscher and G.Fettweis, "Digital compensation of transmitter leakage in FDD zero-IF receivers," *Trans. Emerg. Tel. Tech*, vol. 23, no. 2, pp. 105–120, 2012.

[14] W.Schacherbauer, T.Ostertag, C. C. W.Ruppel *et al.*, "An Interference Cancellation Technique for the Use in Multiband Software Radio Frontend Design," in *Microw. Conf. 2000. 30th Eur.*, 2000, pp. 1–4.

[15] S.Kannangara and M.Faulkner, "Analysis of an Adaptive Wideband Duplexer With Double-Loop Cancellation," *Veh. Technol. IEEE Trans.*, vol. 56, no. 4, pp. 1971–1982, 2007.

[16] D. W.Bliss, T. M.Hancock, and P.Schniter, "Hardware phenomenological effects on cochannel full-duplex MIMO relay performance," in *Signals, Syst. Comput. (ASILOMAR), 2012 Conf. Rec. Forty Sixth Asilomar Conf.*, 2012, pp. 34–39.

[17] B. P.Day, A. R.Margetts, D. W.Bliss *et al.*, "Full-Duplex MIMO Relaying: Achievable Rates Under Limited Dynamic Range," *Sel. Areas Commun. IEEE J.*, vol. 30, no. 8, pp. 1541–1553, 2012.

[18] T.Riihonen and R.Wichman, "Analog and digital self-interference cancellation in full-duplex MIMO-OFDM transceivers with limited resolution in A/D conversion," in *Signals, Syst. Comput. (ASILOMAR), 2012 Conf. Rec. Forty Sixth Asilomar Conf.*, 2012, pp. 45–49.

[19] A.Sahai, G.Patel, C.Dick *et al.*, "Understanding the impact of phase noise on active cancellation in wireless full-duplex," in *Signals, Syst. Comput. (ASILOMAR), 2012 Conf. Rec. Forty Sixth Asilomar Conf.*, 2012, pp. 29–33.

[20] A.Sahai, G.Patel, and A.Sabharwal, "Asynchronous full-duplex wireless," in *Commun. Syst. Networks (COMSNETS), 2012 Fourth Int. Conf.*, 2012, pp. 1–9.

[21] S.Barghi, A.Khojastepour, K.Sundaresan *et al.*, "Characterizing the throughput gain of single cell MIMO wireless systems with full duplex radios," in *Model. Optim. Mobile, Ad Hoc Wirel. Networks (WiOpt), 2012 10th Int. Symp.*, 2012, pp. 68–74.

[22] J.Hyungsik, L.Sungmook, K.Dongkyu *et al.*, "Full Duplexity in Beamforming-Based Multi-Hop Relay Networks," *Sel. Areas Commun. IEEE J.*, vol. 30, no. 8, pp. 1554–1565, 2012.

[23] P.Radunovic, Bozidar; Gunawardena, Dinana; Proutieri, Alexandre; Singh, Nikhil; Balan, Vlad; Key, "Effciency and Fairness in Distributed Wireless Networks Through Self-interference Cancellation and Scheduling," 2009. [Online]. Available: http://research.microsoft.com/pubs/79933/msr-tr-2009-27.pdf

[24] E.Everett, M.Duarte, C.Dick *et al.*, "Empowering full-duplex wireless communication by exploiting directional diversity," in *Signals, Syst. Comput. (ASILOMAR), 2011 Conf. Rec. Forty Fifth Asilomar Conf.*, 2011, pp. 2002–2006.

[25] E.Everett, A.Sahai, and A.Sabharwal, "Passive Self-Interference Suppression for Full-Duplex Infrastructure Nodes," *Wirel. Commun. IEEE Trans.*, vol. 13, no. 2, pp. 680–694, 2014.

[26] C.Jung Il, S.Hong, M.Jain *et al.*, "Beyond full duplex wireless," in

Signals, Syst. Comput. (ASILOMAR), 2012 Conf. Rec. Forty Sixth Asilomar Conf., 2012, pp. 40–44.

[27] M. A.Khojastepour, K.Sundaresan, S.Rangarajan *et al.*, "The case for antenna cancellation for scalable full-duplex wireless communications," in *Proc. ACM Work. Hot Top. Netw.*, Cambridge, MA, 2011.

[28] T.Riihonen, S.Werner, and R.Wichman, "Mitigation of Loopback Self-Interference in Full-Duplex MIMO Relays," *Signal Process. IEEE Trans.*, vol. 59, no. 12, pp. 5983–5993, 2011.

[29] N.Phungamngern, P.Uthansakul, and M.Uthansakul, "Digital and RF interference cancellation for single-channel full-duplex transceiver using a single antenna," in *Electr. Eng. Comput. Telecommun. Inf. Technol. (ECTI-CON), 2013 10th Int. Conf.*, 2013, pp. 1–5.

[30] S. H.Abdelhalem, P. S.Gudem, and L. E.Larson, "Hybrid Transformer-Based Tunable Differential Duplexer in a 90-nm CMOS Process," *Microw. Theory Tech. IEEE Trans.*, vol. 61, no. 3, pp. 1316–1326, 2013.

[31] M.Mikhemar, H.Darabi, and A. A.Abidi, "A Multiband RF Antenna Duplexer on CMOS: Design and Performance," *Solid-State Circuits, IEEE J.*, vol. 48, no. 9, pp. 2067–2077, 2013.

[32] H.Darabi, A.Mirzaei, and M.Mikhemar, "Highly Integrated and Tunable RF Front Ends for Reconfigurable Multiband Transceivers: A Tutorial," *Circuits Syst. I Regul. Pap. IEEE Trans.*, vol. 58, no. 9, pp. 2038–2050, 2011.

[33] M.Mikhemar and H.Darabi, "Rf Front End With On-Chip Transmitter/Receiver Isolation And Noise Matched LNA," U.S. Patent 8 208 865, June, 2012.

[34] P.Pursula, I.Marttila, and K.Nummila, "Wideband adaptive isolator for UHF RFID reader," *Electron. Lett.*, vol. 45, no. 12, pp. 636–637, 2009.

[35] P.Pursula and H.Seppa, "Hybrid Transformer-Based Adaptive RF Front End for UHF RFID Mobile Phone Readers," in *RFID, 2008 IEEE Int. Conf.*, 2008, pp. 150–155.

[36] M.Mikhemar, H.Darabi, and A.Abidi, "An on-chip wideband and low-loss duplexer for 3G/4G CMOS radios," in *VLSI Circuits (VLSIC), 2010 IEEE Symp.*, 2010, pp. 129–130.

[37] ——, "A tunable integrated duplexer with 50dB isolation in 40nm CMOS," in *Solid-State Circuits Conf. - Dig. Tech. Pap. 2009. ISSCC 2009. IEEE Int.*, 2009, pp. 386–387,387a.

[38] H. J.Carlin and A. B.Giordano, *Network theory: an introduction to reciprocal and non-reciprocal circuits*. Prentice-Hall, 1964. [Online]. Available: http://books.google.co.uk/books?id=brc8AAAAIAAJ

[39] R.Vaughan, J. B.Andersen, and I. o. E.Engineers, *Channels, propagation and antennas for mobile communications*. Institution of Electrical Engineers, 2003. [Online]. Available: http://books.google.co.uk/books?id=nAFTAAAAMAAJ

Leo Laughlin graduated from the University of York, UK, in 2011 with an M.Eng degree in Electronic Engineering and was awarded prizes for best M.Eng student and best project in Radio Frequency Engineering. In 2009/10 he completed a 12 month industrial placement at Qualcomm (UK), developing system level simulations for Evolved EDGE receivers in mobile handsets and creating software tools for debugging receiver chains in hardware prototype modems. In 2011 Leo was with Omnisense Ltd, Cambridge, UK, characterising receiver performance in radio geolocation systems and developing signal processing algorithms for human fall detection. Leo is currently a Ph.D Student at the University of Bristol. His research interests are in the area of In-band Full-duplex wireless and flexible radio architectures for LTE handsets.

Mark A. Beach is a Professor in Radio Systems Engineering at the University of Bristol (UK). He is recognised for his research in the field of wireless communications, with specialisation in the field of multi-antenna technology for enhanced efficiency and robust wireless delivery as well as RF enabling technologies for spectrum and energy efficient connectivity. He has held the post of Head of Electrical and Electronic Engineering at Bristol and now is the UK representative on EU COST IC1004, member of the EPSRC Strategic Advisory Team (SAT) for ICT and manages the CDT in Communications at Bristol.

Kevin A. Morris received his B.Eng. and Ph.D. degrees in electronics and communications engineering from the University of Bristol in 1995 and 1999 respectively. He currently holds the post of Reader in Radio Frequency Engineering within the Department of Electrical and Electronic Engineering at the University of Bristol. Currently he is involved with a number of research programmes within the U.K. He has authored or co-authored 60 academic papers and is the joint author of 5 patents. His research interests are principally in looking at methods of reducing power consumption in communications systems including the area of radio frequency hardware design with specific interest in the design of efficient linear broadband power amplifiers for use within future communications systems.

John L. Haine graduated with B.Sc (1971) and Ph.D (1977) degrees from Birmingham and Leeds Universities in the UK. He has worked on wireless R&D for a number of companies including start-ups, focusing mainly on air interface and circuit aspects, as well as being involved in a number of standards and M&A activities. He is currently responsible for RF technology strategy in u-blox AG, working on new standards for IoT communications and looking at key cellular RF implementation technologies. He is a member of the IEEE and IET, and serves on the Board of Cambridge Wireless.